# ESTIMATING WATER FLOW THROUGH A HILLSLOPE USING THE MASSIVELY PARALLEL PROCESSOR

J. E. Devaney
Science Applications Research
Lanham, Maryland

P. J. Camillo and R. J. Gurney
NASA/Goddard Space Flight Center
Greenbelt, Maryland

ABSTRACT

A new two-dimensional model of water flow in a
hillslope has been implemented on the Massively
Parallel Processor at GSFC. Flow in the soil both
in the saturated and unsaturated zones, evaporation
and overland flow are all modelled, and the
rainfall rates are allowed to vary spatially.
Previous models of this type had always been very
limited computationally. This model takes less
than a minute to model all the components of the
hillslope water flow for a day. The model can now
be used in sensitivity studies to specify which
measurements should be taken and how accurate they
should be to describe such flows for environmental
studies.

## INTRODUCTION

One important part of the global hydrological
system is a catchment, which separates rainfall
into evaporation, overland flow, and infiltration.
For a heavy rain, infiltration excess reaches the
stream first as overland flow. Part of the
infiltrated water may then flow rapidly below the
surface to re-emerge downslope or enter the stream.
This is usually referred to as saturated subsurface
flow. The rest reaches the unsaturated zone. The
flow there is vertical and horizontal, and the
latter component may eventually contribute to the
stream flow. Another component which can
contribute to the stream flow is horizontal flow in
a perched water table above the bedrock.

The primary output of catchment models is the
hydrograph, in which the rainfall and fluxes to
the stream from each of the above processes are
plotted as a function of time. The rainfall
rate and the sum of all the output fluxes are the
usual data from a catchment, and a primary goal of
catchment modelling is to understand the
sensitivity of the output to the physical
characteristics of the catchment, such as
topography, cover type, soil characteristics, and
antecedent moisture.

Ref. 13 define catchment models as being of three
basic types, but with overlapping characteristics
so they may be considered a continuum. The first
is stochastic. These models are statistical, in
which time series of measured hydrographs (output)
are correlated to rainfall (input) using classical
time series analysis techniques. This leads quite
naturally to parametric models, their second class,
in which the parameters of the stochastic models
are related empirically to the physical properties

of the catchment. The third class contains
deterministic models based on the laws of
conservation of energy, mass, and momentum, usually
expressed as time and space dependent differential
equations. As these almost always contain non-
measurable parameters which must be calibrated,
deterministic models are partly parametric.

There are many deterministic catchment models, but
none of them includes all of the processes in the
hydrological cycle. In part this is because we
don't even know what they all are, due to the
extreme complexity and variability of natural
catchments. However, no existing model even
includes all the processes previously
described, because no serial computer can model
them with a reasonable amount of computer time for
a spatially variable catchment and for a long
enough time period (Ref. 1,7,8,13.15).

The concept of partial (or contributing) areas is
one basis of our understanding of how catchments
distribute rainfall (Ref. 17). Due to the spatial
variability of catchment characteristics (soils,
cover, topography), different areas handle the rain
in different ways. For example, if the rain rate
exceeds the infiltration capacity for a particular
area, then the excess rain becomes overland flow.
Once the soil is saturated, the water can flow
rapidly below the surface and parallel to it. This
process is referred to as saturated subsurface
flow. The water will re-emerge somewhere
downslope, adding to overland flow. The areas
change over time, so the saturated partial area
which contributes to overland flow varies in time
as well as in space.

We have tried to overcome the computing limitations
by developing a model on the Massively Parallel
Processor (MPP). The model consists of a set of
partial differential equations, solved in parallel,
and so adapts naturally to a parallel architec-
ture. The MPP hillslope model includes the
following components:

-- Surface retention

-- A complete surface energy balance (tempera-
   ture and moisture) with separate evaporation
   rates from the soil, plants (with water
   extraction from the unsaturated zone), and
   surface retention

-- Overland flow

-- Saturated subsurface flow parallel to the
   surface

-- Horizontal and vertical flow in the unsatur-
ated zone

-- Horizontal flow in an unconfined aquifer

Our model is a vertical slice of a hillslope, so it
is basically a two-dimensional model. It may be
considered three-dimensional only if the gradients
are all downslope, not across the slope. It is
based on a catchment model of Ref. 11, which is
simply a series of uncoupled one-dimensional soil
columns placed side by side. We have improved
their design by allowing for horizontal flow in the
unsaturated zone between the columns, and including
the soil and surface temperatures.

We decided at the beginning of this research effort
to create one-, two-, and then three-dimensional
models in succession. The one-dimensional model
(Ref. 6) was compared to a similar one which runs
on a serial machine (Ref. 5,10) to make sure the
equations are solved correctly on the MPP, and as a
timing benchmark. After the two-dimensional model
is completely tested, we plan to develop a three-
dimensional version.

Our use of a parallel processor significantly
reduces the execution time. Typically a 24 hour
period may be modeled in about one CPU minute.
Ref. 11 state that their model does not use
excessive computer time on a serial machine, but
they only present results from 6 hour simulations.

THE TWO-DIMENSIONAL MODEL

The specifications for each of the components of
the model given in the first section are described
here as flux and continuity partial differential
equations. The method of solution is also briefly
described.

Unsaturated Zone

Moisture flow is modeled as described in Ref. 5,
except we now have a horizontal component in the
soil moisture flux. The surface temperature is
modeled by the force-restore method.

Boundary value fluxes must be specified for
moisture at the top and bottom of the hillside
(vertical direction) and at the hillslope divide
and surfaces (horizontal direction). The top
boundary flux is the infiltration or evaporation
rate, computed from the surface energy balance.
The horizontal flux into the hillslope at the
divide is zero. The horizontal flux at the
hillslope surface depends on whether that cell is
saturated. If it is and the sum of the vertical
fluxes plus the horizontal flux into the cell from
the interior of the hillslope would cause soil
moisture to exceed saturation, then the flux onto
the surface is set to whatever value is needed to
keep moisture just as saturation. Otherwise, it is
zero. This is the mechanism which allows
subsurface return flow.

Saturated Zone

The water table height in each column is HB. The
horizontal flux is QB, and the vertical flux is QZ.
The fluxes and vertical boundary conditions are
calculated by the one dimensional Boussinesq
equation (Ref. 14). The flux into the water table
from the unsaturated zone is modelled as the
vertical hydraulic conductivity of the layer, and
the bottom boundary condition is an input parameter
representing an impervious layer or upward or
downward seepage.

The flux at the catchment divide is set to zero.
At the seepage face the height HB is a fixed input
parameter. Therefore the time derivation of HB is
zero for the last column, and the discretized form
of this derivative may be solved for the horizontal
flux at the seepage face. This is the saturated
zone flux which contributes to the hydrograph.

Overland Flow

If the surface water height is larger than a
critical value, the overland flow flux is
determined by Manning's equation (Ref. 7).

The infiltration rate is basically the Green-Ampt
model (Ref. 9), with the usual modification which
replaces the depth of the wetting front with the
cumulative infiltration:

$$I(t) = a + b / \int_0^t I(t') \, dt' \qquad (1)$$

Surface Energy Balance

The energy balance equation provides the surface
fluxes:

$$G = R + LE + LH \qquad (2)$$

All fluxes are positive downward. G is the heat
absorbed by the soil, R is the net radiation flux,
LE is the evapotranspiration energy flux, and H is
the sensible heat. After finding the solution, the
surface moisture flux $q_\theta$ is set equal to the soil
evaporation rate, and G is used in the force-
restore model. The surface temperature needed to
evaluate the fluxes is known from the force-restore
equation. The latent and sensible heat fluxes are
the usual resistance formulations. We imagine the
soil and vegetation as one surface with the
temperature $T_s$. We also allow for some surface
water storage. This affects the evaporation rates,
because the surface resistance is zero for the
fraction of the evaporation which comes from the
stored water.

Method of Solution

The soil moisture and temperature continuity
equations are solved by calculating the spatial
derivatives of the moisture fluxes and then
computing the time integral using numerical models.

The soil is divided into cells by creating a grid
of N layers and M columns of varying widths $\Delta z_i$ and
$\Delta x_i$ respectively, which are input parameters. At a
specified time the fluxes at the interior

250

boundaries are calculated. The surface energy balance equations are evaluated and all boundary conditions applied. The continuity equations are of the form:

$$\frac{d\vec{y}}{dt} = \vec{f}(t,y) \qquad (3)$$

The vector y represents the state of the system in the unsaturated zone and $\vec{f}(t,y)$ represents the model equations. This is solved with an Adams-Bashforth predictor-corrector method (Ref. 3,16). This solution is described in detail in Ref. 5. Since double precision is not available on the MPP, the form of the predictor-correction equations with the calculations done with the derivatives instead of the backward differences was used. New values of the state vector, $\vec{y}(p)(t+\Delta t)$ are predicted in terms of the previous derivatives. The derivatives are recalculated from the model equations, and then the corrected value of the state vector, $\vec{y}(c)(t+\Delta t)$, is obtained.

The difference between $\vec{y}(p)$ and $\vec{y}(c)$ is a reliable estimate of the discretization error, and the software determines if each element of this difference lies within a user-specified window. If all differences are smaller than this window, the integration step size ($\Delta t$) is doubled, leading to increased computational efficiency and reduced roundoff errors. If any difference is too large, the step size is halved. Doubling of the time step was accomplished by saving the previously calculated derivatives and using them. Thus, maximum accuracy could be retained. Where the time step could be doubled because the errors are small enough but there were insufficient back derivatives, doubling was postponed until there were sufficient back data. When the error window checks required that the time step be halved, three of the required derivatives for the predictor-corrector were available, and two were missing. The Runge-Kutta method was used to calculate these needed derivatives. The continuity equations for surface and saturated flow are solved using a Runge-Kutta method throughout.

## UTILIZING THE MPP ARCHITECTURE FOR SPEED

Since identical calculations were needed at each soil cell, the mapping of the two dimensional model of the hillslope was accomplished by assigning an individual processing element to each soil cell (see Fig. 1). Thus, the local memory of each processor contains the values which belong to that cell, i.e. moisture, position, thickness, depth, conductivities, etc. Surface temperature, deep soil temperature, cumulative infiltration, overland flow, and saturated flow were all stored as vectors in the same array as the moisture values since they were part of the state vector.

The first step in the solution required calculation of the fluxes at the interior boundaries of the
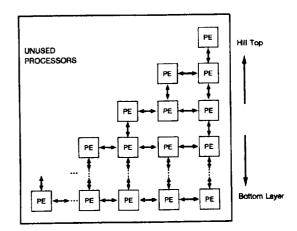


Figure 1.  One processing element is assigned to one soil cell

soil cells. These calculations involved only array arithmetic and nearest neighbor (in one direction for horizontal fluxes and in the other direction for vertical fluxes) calculations. Since the interconnect-scheme of the MPP is a nearest neighbor network, all of the array arithmetic and nearest neighbor calculations could be done in parallel. The next step in the solution required the surface energy balance equations be evaluated and the boundary conditions applied. These all involved vector calculations. Numerous input vectors were required to do these calculations over the course of a model run. Some were time dependent vectors such as the air temperature across the surface of the hillslope throughout the day and some were static throughout the model run, such as surface slope, surface roughness, and surface vegetation properties. These vectors were packed into array columns. To get the vector data to a convenient place to do calculations, the row and column broadcast capability of the MPP was used. This allows fast broadcast of one element from each row (column) to the other processor memories in the same row (column) (see Fig. 2).

It is not necessary that the broadcast row (column) be composed only of elements in a horizontal (vertical) direction but merely that one element per column (row) be selected. The MPP's capability to select arbitrary areas of an array for calculation via boolean masks allowed the completed vector calculation results to be placed for example into the processor memories of only the surface of the hillslope. This combination of data movement via broadcast and boolean selection enabled the vector calculations to be done simply. In addition, since many of the vector calculations were similar, it was possible to do more than one set at a time.

Once the derivatives were calculated, the predictor-corrector equations were used and the differences between them found. The tests on the
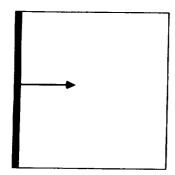
251

Figure 2. The row and column broadcasting
feature of the MPP allows quick
movement of data for vector
calculations

halving (doubling) converted to a hardware
instruction on the MPP and could thus be done in
parallel. This global testing ability of the MPP
was also used to decide if whole blocks of code
needed to be executed or could be skipped. This
occurred for example with the infiltration
calculations under surface saturation. If no part
of the surface was saturated, then these
calculations could be skipped entirely. This also
contributed to the overall speed of execution.

In summary, the program's speed was achieved
through array arithmetic (masked and unmasked),
parallel data movement through nearest neighbor
communication and row and column broadcasting, and
global testing of conditions using 'any' or 'all'
for the purpose of choice in the next set of
calculations. All of these fitted naturally with
the MPP architecture and the computational
requirements of the model. A comparison of the
times (see Table 1) for the model as it has evolved
from a 14 layer, one-dimensional limited flow model
to the current two dimensional model shows that a
single day of data run through the model requires
only about a minute of CPU time.

Table 1. Timing measurements comparing MPP and
a serial processor for 24 hours of data
processed.

One Dimensional Model
(14 soil layers, no rain, vertical flows only)

IBM (Full processing capability):     4 sec
MPP (14/16384 processors):           10 sec

Two Dimensional Model
(102 soil layers, 102 soil columns, horizontal
and vertical unsaturated flows, saturated flow,
overland flow, one hour of rain)

MPP:                                 57 sec

## MODEL OUTPUT

We have not yet completed unit testing of all the
processes in the model. Here we present the
results of one test, which includes the surface
energy balance of and infiltration into an
initially very dry sandy loam soil.

The hillslope is divided into 102 columns of width
.5 meters each. The first column has 100 soil
layers of thickness .1 m and the bottom two layers
.5 meters. The last column has only the bottom two
layers. The slope is a line drawn from the top of
the first column to the top of the last, so the
area modeled is a right triangle with height 11
meters and base 60 meters. These soil cells plus
the additional cells for temperature, infiltration,
overland flow and saturated flow use approximately
one-third of the Array Unit Processor capacity.

The initial volumetric moisture in the unsaturated
zone is set to .05 $m^3 m^{-3}$ everywhere. To model a
sandy loam we have set the parameters in the
hydraulic conductivity and matric potential models
to $\theta_s$ = .375, $K_s$ = 2.8 x 10$^{-5}$ $m s^{-1}$, $\psi_s$ = -.43 m,
and b = 5. These values were derived from fits to
the characteristic curves measured during an
experiment near Phoenix in 1972 (Ref. 12). They
were reused for each of the 6 days modeled here.
Ref. 4 show how these data were fitted to the
surface energy balance model. The rainfall rate
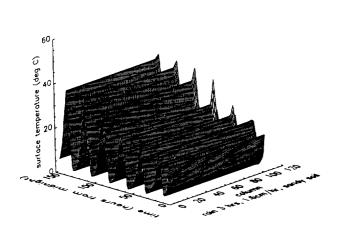was          1.6 cm h$^{-1}$ for the first 3 hours.

Perhaps the most important result is that the
simulations took approximately 1 minute of CPU time
per 24 hour period, or 6 minutes for the entire 6
day run. In numerical simulations on earth science
problems, computer runs of an hour or more are not
uncommon. In such a time, it is feasible to
simulate 2 months or more of model time on the MPP.
This will allow for simulations of many storms and
inter-storm periods.

Figure 3a and 3b show the force restore solutions
to the surface and deep soil temperatures as
functions of time and column number. Time zero is
the start of the simulation, which here is
midnight. Column 1 is at the hillslope divide
and column 102 is at the seepage face. It is
difficult from these plots to project the daily
maximum value onto the time axis, but for each day
this occurs at 2 p.m. The temperatures range from
22 to 40 ($^o$C), increasing as the soil surface
dries. The temperatures in the last three columns
show some problems, which we are examining.

Figure 4a shows soil moisture in the top soil layer
as a function of time and position. The rapid rise
as the initially dry soil absorbs all the rain and
the subsequent decline over the next 5 days are
physically realistic.

Figure 4b shows the soil moisture profile in column
50 (halfway down the hillslope) as a function of
time. This shows that the moisture never
penetrates deeper than the top 5 layers, or .5
meters. It also shows that after 2 days the
surface exhibits small oscillations about a value
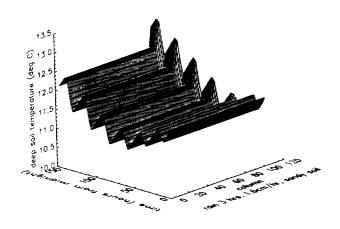of .05 (same as in Fig. 4a), increases to a value

Figure 3a.  Force-restore solution for the surface
temperature as a function of time and
position on the hillslope



Figure 4a.  Surface soil moisture as a function
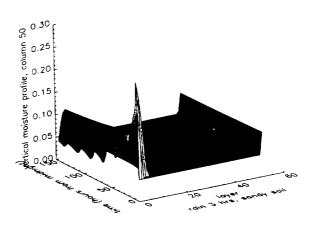of time and position on the hillslope



Figure 3b.  Force-restore solution for the deep
soil temperature as a function of
time and position on the hillslope



Figure 4b.  Soil moisture profile for column 50 as
a function of time

of about .12 at about .3 meters then decreases to
an unchanging value of .05 below .5 meters.  Thus,
the dynamic zone seems to be the top .5 meters.

Figure 4c shows the variation of the top cell soil
moisture as a function of time.  The effects of
infiltration and evaporation, as well as of
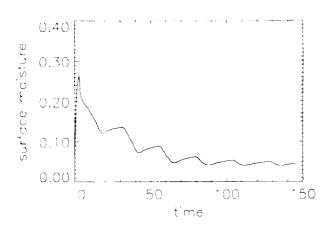capillary action, can be seen.

Figure 5a shows the infiltration rate as a function
of time and position.  The maximum rate shown here
($4.4 \times 10^{-4}$ cm s$^{-1}$) equals the rain rate, 1.6 cm
h$^{-1}$.  Figure 5b shows the cumulative evaporation
everywhere as 4.8 cm, exactly equal to the
cumulative rainfall.  For this simulation, then,
all the rain immediately infiltrated into the soil
surface.  Figure 5b also shows that the cumulative
infiltration calculation is correct.  There is no
surface retention.

radiation, a rather large value. The problem is not in the values for thermal conductivity and heat capacity, as may be seen in Figure 7. These vary with soil moisture as they should.



Figure 4c.  Surface moisture for column 50 as a function of time
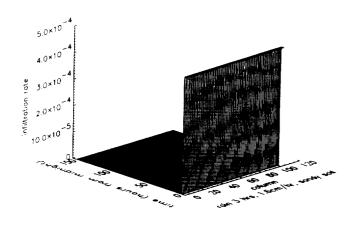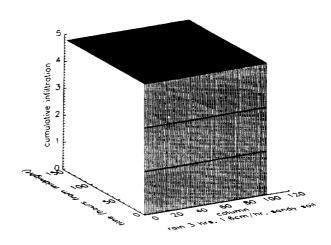


Figure 5b.  Cumulative infiltration as a function of position and time



Figure 5a.  Infiltration rate as a function of position and time

The surface energy balance fluxes are plotted in Figs. 6a-6d. The net radiation (Fig. 6a) is the data used to drive the energy balance model. These are the same very day, as we simply reused the 24 hour data set each day. The latent heat flux (Fig. 6b) decreases each day as the soil dries out. The sensible heat flux (Fig. 6c) exhibits peculiar behavior, being predominantly positive (towards the soil in the sign convention of Eq. 2) for the first 4 days and negative thereafter. Finally, Figure 6d shows the soil heat flux. It is positive during the day as it should be for a soil surface which is getting warmer every day, but it is also 50% of net
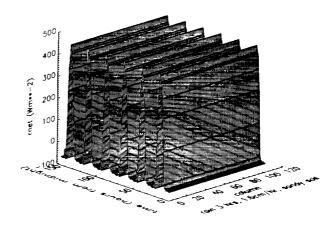


Figure 6a.  Surface net radiation as a function of time and position

These peculiarities in the surface fluxes are most likely due to the use of the same net radiation every day, which cannot be representative of all the surface conditions modeled here. This is being checked out by using modeled instead of measured radiation.
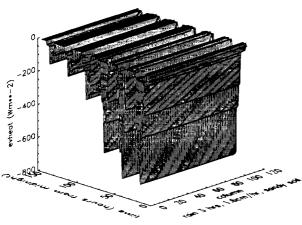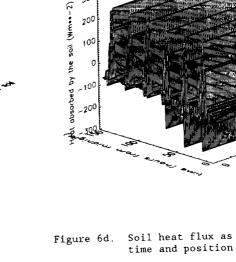
Figure 6b.  Latent heat flux as a function of
time and position



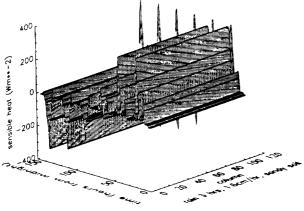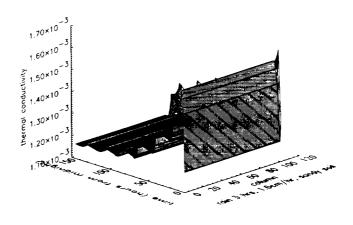Figure 6d.  Soil heat flux as a function of
time and position



Figure 6c.  Sensible heat flux as a function of
time and position



Figure 7a.  Thermal conductivity of the top soil
layer as a function of time and
position

## SUMMARY

We have presented a new model of the hydrological
response of a hillslope to rain.  It runs on a SIMD
parallel architecture computer, the Massively
Parallel Processor, at Goddard Space Flight Center.
Its major advantage over other models of its type
is its much reduced execution times (due to the
parallel architecture of the MPP) from what one
gets on a serial machine.  This allows the model to
include more of the hydrological processes than any
other model has been able to, including saturated
subsurface flow and a sophisticated surface energy
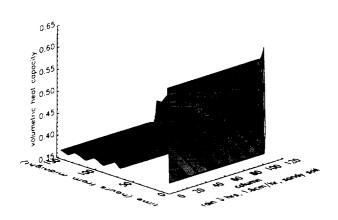balance.

Figure 7b.   Heat capacity of the top soil layer
              as a function of time and position

REFERENCES

1.  Bathurst, J. C., "Physically-based Distributed
    Modeling of an Upland Catchment Using the
    Systeme Hydrologique Europeen," Institute
    of Hydrology, Wallingford, Oxon, UK.

2.  Becker, F., P. J. Camillo and B. Choudhury,
    "Review of ET Estimation by Means of Satellite
    Data," Proceedings of the ISLSCP Conference on
    Satellite Data Algorithms, Pasadena, CA,
    January 1987.

3.  Devaney, J. E., P. J. Camillo and R. J. Gurney,
    "A SIMD Implementation of a One-Dimensional
    Energy-Moisture Balance Model," submitted to
    Proceedings of the ISLSCP Conference on
    Satellite Data Algorithms, Pasadena, CA,
    January 1987.

4.  Booth, A. D., Numerical Models, Academic Press,
    New York, 1957.

5.  Camillo, P. J. and R. J. Gurney, "A Resis-
    tance Parameter for Bare Soil Evaporation
    Models," Soil Science, 141, 1986, 95-105.

6.  Camillo, P. J., R. J. Gurney and T. J.
    Schmugge, "A Soil and Atmospheric Boundary
    Layer Model for Evapotranspiration and
    Soil Moisture Studies," Water Resources
    Research, 19, 1983, 371.

7.  Devaney, J. E., P. J. Camillo and R. J.
    Gurney, "A SIMD Implementation of a
    Distributed Watershed Model," Proceedings
    of the Second International Conference on
    Supercomputing, Santa Clara, California,
    May 3-8, 1987.

8.  Eagleson, P. S., Dynamic Hydrology,
    McGraw-Hill, New York, NY, 1970.

9.  Freeze, R. A., "Three-Dimensional, Transient,
    Saturated-Unsaturated Flow in a Groundwater
    Basin, Water Resources Research, 7, 1971,
    929-941.

10. Green, W. A. and H. A. Ampt, Studies on
    Soil Physics, 1. The Flow of Air and Water
    Through Soils, Journal of Agricultural Soils,
    4, 1911, 1-24.

11. Gurney, R. J. and P. J. Camillo, "Modelling
    Daily Evaporation Using Remotely Sensed
    Data," Journal of Hydrology, 69, 1984, 305-324.

12. Hillel, D. and G. M. Hornberger, "Physical
    Model of the Hydrology of Sloping Heterogeneous
    Fields," Soil Science Soc. Am. J., 43, 1979,
    434-439.

13. Jackson, R. D., "Diurnal Changes in Soil-Water
    Content During Drying," in Field Soil Water
    Regime, R. R. Bruce et al. (eds.), Soil Sci.
    Soc. Am. Proc, Special Publ. 5, 1973.

14. Kirkby, M. J. (ed.), Hillslope Hydrology,
    Wiley-Interscience, Chichester, UK, 1972.

15. Pikul, M. F., R. L. Street, I. Remson, "A
    Numerical Model Based on Coupled One-Dimen-
    sional Richard and Boussinesq Equations,"
    Water Resources Research, 10, 1974, 295-302.

16. Smith, R. E. and D. A. Woolhiser, "Overland
    Flow on an Infiltrating Surface, Water
    Resources Research, 7, 1971, 899-913.

17. Teddington, A., Modern Computing Methods,
    Philosophical Library, New York, 1958.

18. van de Griend, A. A. and E. T. Engman,
    "Partial Area Hydrology and Remote Sensing,"
    Journal of Hydrology, 81, 211-251.